ECC
Eurasian Chemical Communications
Original Research Article
http://echemcom.com

Phosphotungstic acid supported on functionalized graphene oxide nanosheets (GO-SiC_3-NH_3-H_2PW): Preparation, characterization, and first catalytic application in the synthesis of amidoalkyl naphthols

Zahra Hoseini[a], Abolghasem Davoodnia[a,*], Amir Khojastehnezhad[b], Mehdi Pordel[a]

[a]*Department of Chemistry, Mashhad Branch, Islamic Azad University, Mashhad, Iran*

[b]*Young Researchers and Elite Club, Mashhad Branch, Islamic Azad University, Mashhad, Iran*

Received: 23 September 2019, Accepted: 15 November 2019, Published: 02 December 2019

Abstract

Grafting of 3-aminopropyltriethoxysilane (APTS) on graphene oxide (GO) nanosheets followed by reaction with phosphotungstic acid ($H_3PW_{12}O_{40}$, denoted as H_3PW) gave a new functionalized GO which was characterized using FT-IR, FESEM, EDX, EDX elemental mapping and ICP-OES techniques. The catalytic activity of this nanomaterial containing phosphotungstic counter-anion $H_2PW_{12}O_{40}^-$ (H_2PW) which was denoted as GO-SiC_3-NH_3-H_2PW was probed in the synthesis of amidoalkyl naphthols through the one-pot, three-component reaction of β-naphthol with various aromatic aldehydes and acetamide. The results showed a significant catalytic performance of the catalyst for this transformation in ethanol as solvent at reflux temperature, giving the corresponding products in high yields. In addition, the nanocatalyst could be easily recovered from the reaction mixture and reused many times with no significant loss of its catalytic activity.

Keywords: Phosphotungstic acid; $H_3PW_{12}O_{40}$; functionalized graphene oxide; amidoalkyl naphthols.

Introduction

Graphene which is a two-dimensional monolayer of carbon atoms can be arranged in a honeycombed network. Graphene-based nanosheets have attracted much attention in recent years owing to their unique properties such as high thermal conductivity, extremely high surface area, thermal and chemical stability, good biocompatibility, and good mechanical strength [1-4]. These features make graphene-base materials appropriate for use in various fields such as electrochemical sensors and biosensors [5-8], anti-cancer drugs delivery [9], catalyst in degradation of methylene blue [10], detection of neurotransmitters [11], energy technology [12], in microsupercapacitor [13], and cell biotechnology [14]. Recently, graphene oxide (GO) that can be easily prepared from graphite powder

*Corresponding author: Abolghasem Davoodnia
Tel: +98 (51) 38435000, Fax: +98 (51) 38429520
E-mail: adavoodnia@mshdiau.ac.ir; adavoodnia@yahoo.com

using Hummers method [15,16] and converted to graphene by reduction using reducing agents such as $NaBH_4$ [17] or hydrazine [18], has also attracted great interest as a new low-cost carbocatalytic material with remarkable potential to facilitate various chemical transformations [19-22]. Functionalization of GO is necessary for various applications such as carbocatalysis. The presence of hydrophilic oxygen-containing groups on the surface of GO nanosheets such as hydroxyl, epoxy, and carboxyl groups makes the surface modification of GO with a better efficiency and allows construction of various novel functional groups attached at the GO surface [23-26]. The methods for covalent functionalization of GO include amidation reaction between the carboxylic acid group of GO and amine [27], esterification reaction between the carboxylic acid group of GO and hydroxyl group in alcohol compounds [28], reaction between the hydroxyl and carboxyl groups of GO and isocyanates [29], and silylation of the hydroxyl groups of GO using 3-aminopropyltriethoxysilane (APTS), as a silane coupling agent [30,31].

Multicomponent reactions (MCRs) have gained considerable attention as a powerful method in organic synthesis and medicinal chemistry because they involve simultaneous reaction of more than two starting materials to yield a single product through one-pot reaction [32-34]. Development of new MCRs and improvement and modification of the known MCRs are still popular areas of research in current organic chemistry [35-37]. One such reaction is the synthesis of amidoalkyl naphthols which are generally synthesized *via* the three-component reaction of *β*-naphthol with an aldehyde and an amide in the presence of various promoting agents [38-46].

Based on these precedents and in line with our interest in catalysis [47-55], herein, we report the preparation of a new functionalized GO containing a phosphotungstic counter-anion $H_2PW_{12}O_{40}$ (H_2PW) by grafting of APTS on GO nanosheets followed by a reaction with phosphotungstic acid ($H_3PW_{12}O_{40}$, denoted as H_3PW) which was fully characterized (Scheme 1). The catalytic activity of this new material which was denoted as GO-SiC_3-NH_3-H_2PW was then investigated in one-pot synthesis of amidoalkyl naphthols by reaction of *β*-naphthol, aromatic aldehydes, and acetamide (Scheme 2).

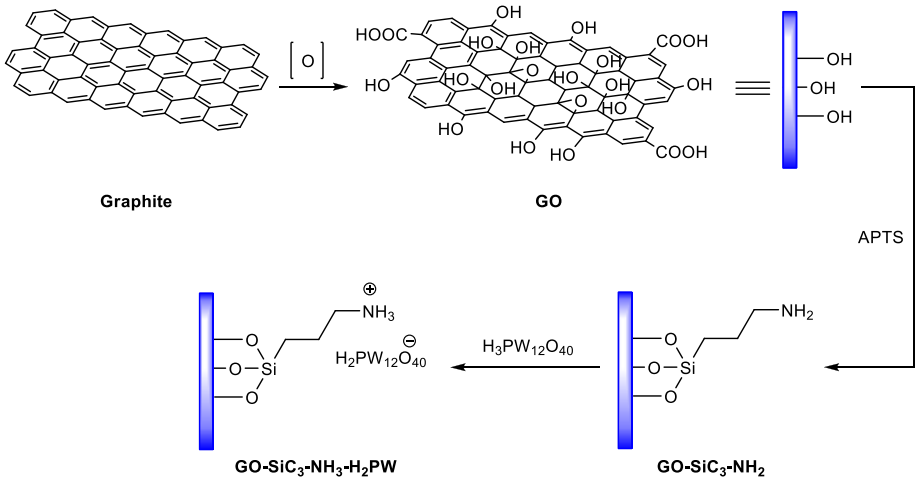

Scheme 1. Preparation of GO-SiC_3-NH_3-H_2PW nanosheets

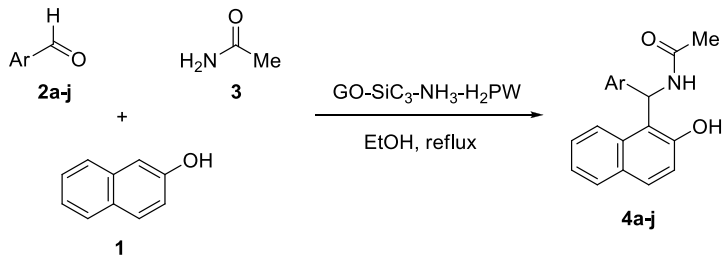

Scheme 2. Synthesis of amidoalkyl naphthols in the presence of GO-SiC_3-NH_3-H_2PW nanosheets

Experimental

All chemicals were purchased from Merck and Aldrich and used without further purification. Melting points were recorded with a Stuart SMP3 melting point apparatus. Fourier transform infrared (FT-IR) spectra were obtained using a Tensor 27 Bruker spectrophotometer as KBr disks. Ultrasonication was performed using a Soltec sonicator at a frequency of 40 kHz and a nominal power of 260 W. Field emission scanning electron microscopy (FESEM) analyses were done using a TESCAN BRNO-MIRA3 LMU. Energy-dispersive X-ray (EDX) analysis and elemental mapping were performed using a SAMX model instrument. The amount of phosphorus and tungsten in the catalyst was determined using inductively coupled plasma optical emission spectroscopy (ICP-OES) conducted with a Spectro Arcos model spectrometer. The ^1H NMR (300 MHz) spectra were recorded on a Bruker 300 FT spectrometer, in DMSO-d_6 as the solvent using tetramethyl silane (TMS) as internal standard.

Preparation of GO nanosheets

GO nanosheets were prepared from natural graphite using Hummers method [15] with some modification. A mixture of graphite powder (5.0 g), sodium nitrate ($NaNO_3$, 2.5 g), and concentrated sulfuric acid (115 mL, 98% H_2SO_4) was stirred in an ice bath at 0-5 °C for 15 min and, then, potassium permanganate ($KMnO_4$,15.0 g) was slowly added. The stirring was continued for 2 h while the temperature was kept in the range of 0-10 °C. The mixture was then transferred to a water bath and stirred at 35 °C for 30 min, forming a brownish grey thick paste. Afterwards, deionized water (230 mL) was slowly added to the paste and the suspension, now brown in color, was stirred at 95-98 °C for 15 min. The suspension was further diluted with warm deionized water (700 ml, 40 °C), followed with a drop by drop addition of 30% hydrogen peroxide (H_2O_2, 50 mL). The mixture was centrifuged and the isolated yellow-brown cake was washed with diluted HCl (5 wt%) and deionized water several times until the pH became neutral. The solid graphite oxide was separated by centrifugation and dried at 60 °C under vacuum for 12 h. The obtained graphite oxide (0.4 g) was dispersed in distilled water (400 mL) and sonicated in an ultrasonic bath cleaner (100 W) for 1 h to exfoliate graphitic oxide. The complete exfoliation of graphite oxide is confirmed with the formation of light brown coloured homogeneous dispersion GO. Afterwards, the GO solution was centrifuged for 20 min and then the supernatant was removed (to remove any unexfoliated graphitic oxide). The GO nanosheets were obtained after drying the sediment in a vacuum oven at 80 °C for 24 h.

Preparation of GO-SiC_3-NH_2 nanosheets

GO-SiC_3-NH_2 was prepared by grafting of APTS on GO nanosheets according to methods cited in the literature [30,31]. Briefly, the synthesized GO (1.0 g) was ultrasonically dispersed in anhydrous toluene (30 mL) at room temperature for 30 min and, then, APTS (3.0 mmol, 0.66 g) was added. The mixture was heated under a N_2 atmosphere at 110 °C for 24 h. The resultant solid was filtered and washed with toluene (3 × 10 mL), and dried at 50 °C under vacuum for 24 h to give black powder of GO-SiC_3-NH_2.

Preparation of GO-SiC_3-NH_3-H_2PW

GO-SiC_3-NH_2 (0.5 g) was ultrasonically dispersed in absolute ethanol (10 mL) at 60 °C for 20 min. H_3PW (1.0 mmol, 2.88 g) was added to the suspension and sonication continued for another 1 h at same temperature. The mixture was then refluxed for 12 h. After cooling to room temperature, the solid was collected by filtration and repeatedly washed with absolute ethanol and dried under vacuum at 60 °C for 12 h to form GO-SiC_3-NH_3-H_2PW.

General procedure for the synthesis of amidoalkyl naphthols 4a-j catalyzed by GO-SiC_3-NH_3-H_2PW

A mixture of *β*-naphthol **1** (1.0 mmol, 0.14 g), an aromatic aldehyde **2a-j** (1.0 mmol), acetamide **3** (1.2 mmol, 0.07 g), and GO-SiC_3-NH_3-H_2PW (0.03 g) in ethanol (5 mL) was heated under reflux for 10-20 min. Upon completion of the transformation, monitored by TLC, the reaction mixture was filtered whilst still hot to separate the catalyst. The product was then collected from the filtrate after cooling to room temperature and recrystallized from ethanol to give compounds **4a-j** in high yields. All the products were characterized according to comparison of their melting points with those of authentic samples and for some of them by their FT-IR and ^{1}H NMR spectral data.

Selected FT-IR and ^{1}H NMR data

N-((2-Hydroxynaphthalen-1-yl)(phenyl)methyl)acetamide (4a). ^{1}H NMR (δ, ppm): 1.99 (s, 3H, CH_3), 7.11 (d, *J* = 7.8 Hz, 1H, CH), 7.16 (d, *J* = 8.3 Hz, 2H, H_{Ar}), 7.20-7.34 (m, 5H, H_{Ar}), 7.39 (t, *J* = 7.9 Hz, 1H, H_{Ar}), 7.75-7.87 (m, 3H, H_{Ar} and NH), 8.50 (d, *J* = 8.0 Hz, 1H, H_{Ar}), 10.06 (s br., 1H, OH); FT-IR (*υ*, cm^{-1}): 3439 (NH), 3241 (OH), 1673 (C=O).

N-((4-Chlorophenyl)(2-hydroxynaphthalen-1-yl)methyl)acetamide (4b). ^{1}H NMR (δ, ppm): 2.01 (s, 3H, CH_3), 7.13 (d, *J* = 8.2 Hz, 1H, CH), 7.18 (d, *J* = 8.5 Hz, 2H, H_{Ar}), 7.22-7.35 (m, 4H, H_{Ar}), 7.38 (t, *J* = 7.8 Hz, 1H, H_{Ar}), 7.76-7.87 (m, 3H, H_{Ar} and NH), 8.50 (d, *J* = 8.2 Hz, 1H, H_{Ar}), 10.07 (s, 1H, OH); FT-IR (*υ*, cm^{-1}): 3419 (NH), 3210 (OH), 1685 (C=O).

N-((2-Chlorophenyl)(2-hydroxynaphthalen-1-yl)methyl)acetamide (4d). ^{1}H NMR (δ, ppm): 1.97 (s, 3H, CH_3), 7.13-7.38 (m, 6H, H_{Ar} and CH), 7.42 (t, *J* = 7.2 Hz, 1H, H_{Ar}), 7.62 (dd, *J* = 7.5, 1.3 Hz, 1H, H_{Ar}), 7.73-7.84 (m, 2H, H_{Ar} and NH), 8.06 (d, *J* = 8.6 Hz, 1H, H_{Ar}), 8.64 (d, *J* = 8.0 Hz, 1H, H_{Ar}), 9.89 (s, 1H, OH); FT-IR (*υ*, cm^{-1}): 3414 (NH), 3195 (OH), 1654 (C=O).

N-((2-Hydroxynaphthalen-1-yl)(4-nitrophenyl)methyl)acetamide (4h). ^{1}H NMR (δ, ppm): 1.99 (s, 3H, CH_3), 7.08 (d, *J* = 8.8 Hz, 1H, CH), 7.30 (t, *J* = 7.3 Hz, 1H, H_{Ar}), 7.41-7.50 (m, 2H, H_{Ar}), 7.54 (d, *J* = 8.1 Hz, 1H, H_{Ar}), 7.63-7.83 (m, 5H, H_{Ar}), 7.92 (d, *J* = 8.6 Hz, 1H, NH), 8.65 (d, *J* = 8.2 Hz, 1H, H_{Ar}), 9.79 (s, 1H, OH); FT-IR (*υ*, cm^{-1}): 3374 (NH), 3214 (OH), 1647 (C=O), 1521 and 1347 (NO_2).

N-((2-Hydroxynaphthalen-1-yl)(3-nitrophenyl)methyl)acetamide (4i). ^{1}H NMR (δ, ppm): 2.06 (s, 3H, CH_3), 7.23-7.33 (m, 3H, H_{Ar} and CH), 7.43 (t, *J* = 7.6 Hz, 1H, H_{Ar}), 7.54 (t, *J* = 7.9 Hz, 1H, H_{Ar}), 7.61 (d, *J* = 7.7 Hz, 1H, H_{Ar}), 7.80-7.86 (m, 2H, H_{Ar}), 7.92 (d br., *J* = 8.2 Hz, 1H, NH), 8.03-8.09 (m, 2H, H_{Ar}), 8.68 (d, *J* = 8.0 Hz, 1H, H_{Ar}), 10.19 (s, 1H, OH); FT-IR (υ, cm^{-1}): 3375 (NH), 3223 (OH), 1648 (C=O), 1524 and 1350 (NO_2).

Results and discussion

Preparation and characterization of the catalyst GO-SiC$_3$-NH$_3$-H$_2$PW

GO nanosheets were prepared from natural graphite powder by modified Hummers method [15]. Grafting of APTS on GO nanosheets gave the amino functionalized GO-SiC$_3$-NH$_2$ which was then reacted with H_3PW to afford GO-SiC$_3$-NH$_3$-H$_2$PW as a new functionalized GO containing a phosphotungstic counter-anion. The latter nanomaterial was characterized using FT-IR spectroscopy, FESEM and EDX analysis, EDX elemental mapping, and ICP-OES.

To verify the chemical changes that occurred during the modification of GO, the FT-IR spectra of GO, GO-SiC$_3$-NH$_2$, and GO-SiC$_3$-NH$_3$-H$_2$PW are compared in Figure 1. One intense and broad peak is observed at 3430 cm^{-1} due to the presence of OH groups at the surface of GO (Figure 1(a)) which is the major binding site for amine-functionalized silane material. The adsorption bands at 1716 and 1625 cm^{-1} could be attributed to the carbonyl group of carboxylic acid and stretching vibration of –C=C group of aromatic graphene moiety, respectively. Another characteristic band at 1060 cm^{-1} is related to C-O stretching vibration. Many vibrational peaks in the FT-IR spectrum of GO-SiC$_3$-NH$_2$ (Figure 1(b)) confirm the formation of APTS-coated GO. The vibration peaks at 3427 and 1577 cm^{-1} could be assigned to the amino groups, which revealed the successful grafting of APTS to the GO. The two set of bands at 2927 and 2864 cm^{-1} are attributed to the symmetric and asymmetric methylene groups in alkyl chains moieties. Furthermore, high intense absorption bands at 1053 and 1119 cm^{-1} are assigned to the characteristic absorption of Si-O bonds acquired during the silylation process. Finally, as shown in Figure 1(c), the appearance of the new characteristic peaks at 803 and 1049-1112 cm^{-1} (overlapped with Si-O stretching vibration bands) which originates from the H_2PW stretching vibration bands confirm the successful immobilization of the H_3PW on the organic ligand linked to GO. Other bands in the FT-IR spectrum of GO-SiC$_3$-NH$_3$-H$_2$PW are similar to those of GO-SiC$_3$-NH$_2$ with a slight shift for some of them.

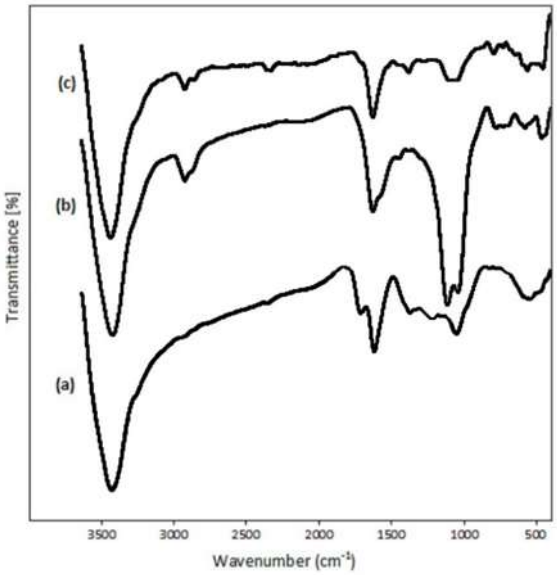

Figure 1. FT-IR spectra of (a) GO, (b) GO-SiC$_3$-NH$_2$, and (c) GO-SiC$_3$-NH$_3$-H$_2$PW

The FESEM analysis was applied for the characterization of GO-SiC$_3$-NH$_3$-H$_2$PW from view point of morphology.

As shown in Figure 2, a nanosheet-like structure in disordered phase with crumpled and wrinkled edges can be seen in FESEM image. These folded edges owing to sp^3-carbon in GO-SiC_3-NH_3-H_2PW, carry SiC_3-NH_3-H_2PW on both sides of the GO nanosheets. These sites may serve as reactive catalytic sites to provide the desired chemical transformation. Many granular-like particles that were distributed on the surfaces of GO sheets in GO-SiC_3-NH_3-H_2PW are also visible, suggesting the organic moieties had bound to the surfaces of the GO nanosheets.

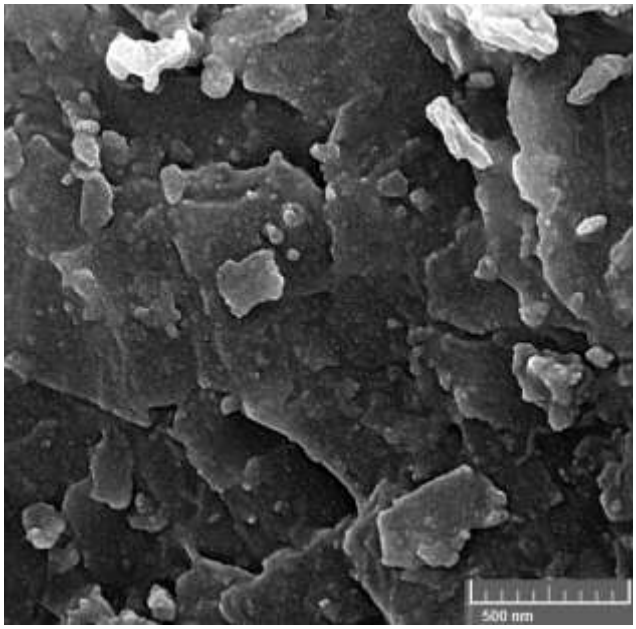

Figure 2. FESEM image of GO-SiC_3-NH_3-H_2PW

Figure 3 displays the EDX spectrum of GO-SiC_3-NH_3-H_2PW, where the signals for carbon, oxygen, silicon, nitrogen, phosphorus, and tungsten with no extra peak related to other impurities confirm the successful functionalization of GO.

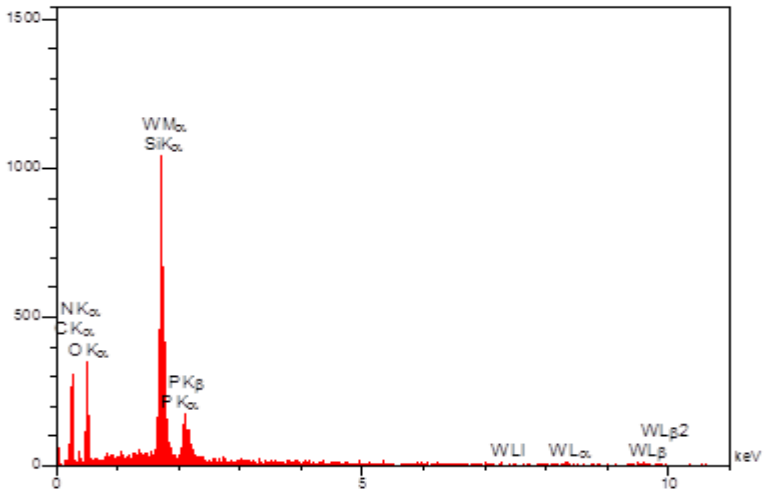

Figure 3. EDX analysis of GO-SiC_3-NH_3-H_2PW

In addition, EDX elemental mapping can provide qualitative information about the distribution of different chemical elements in the catalyst structure. As can be seen in Figure 4, the uniform distribution of Si, N, P, and W, indicates that the functional moieties have uniformly been immobilized on GO, which is very important to perform efficient catalytic organic transformations.

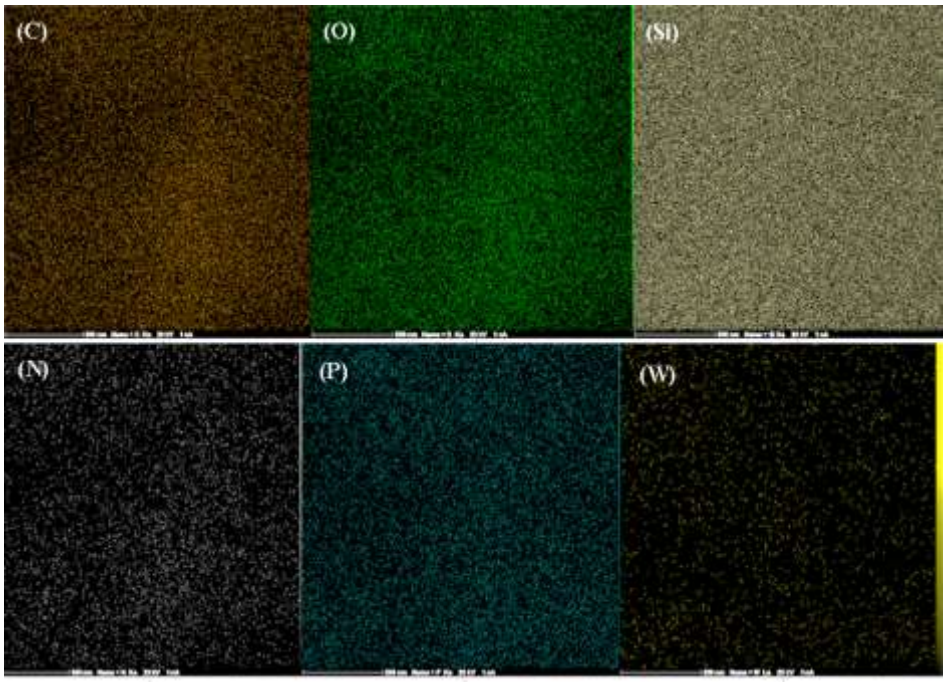

Figure 4. EDX elemental mapping of GO-SiC_3-NH_3-H_2PW

Finally, as determined by ICP-OES, the content of phosphorus and tungsten in the GO-SiC_3-NH_3-H_2PW was 0.100 and 0.525 %, respectively, which is another conformation for immobilization of SiC_3-NH_3-H_2PW over the surfaces of GO nanosheets.

Catalytic evaluation of GO-SiC_3-NH_3-H_2PW in the synthesis of amidoalkyl naphthols

The catalytic activity of the prepared GO-SiC_3-NH_3-H_2PW was tested in the synthesis of amidoalkyl naphthols by one-pot, three-component reaction of *β*-naphthol with various aromatic aldehydes and acetamide. First, to optimize the reaction conditions, the reaction of *β*-naphthol **1** (1 mmol), 4-chlorobenzaldehyde **2b** (1 mmol), and acetamide **3** (1.2 mmol) was investigated as a model in the absence or presence of GO-SiC_3-NH_3-H_2PW as catalyst in different solvents including EtOH, H_2O, EtOH-H_2O, MeOH, CH_3CN, CH_2Cl_2, $CHCl_3$ and also under solvent-free conditions. A summary of the optimization experiments is provided in Table 1. To illustrate the need for catalyst in the reaction, the model reaction was studied in the absence of catalyst in refluxing EtOH, H_2O, or mixture of them and also under solvent-free conditions at high temperature (entries 1-4). The yield of the product was trace even after 120 min. However, when the reaction was performed in the presence of GO-SiC_3-NH_3-H_2PW, the desired product was obtained in moderate to high yields. Ethanol proved to be a much better solvent in terms of yield as well as reaction time than all the others. The excellent yield of the product was obtained when the reaction was

conducted in refluxing EtOH in the presence of 0.03 g of the GO-SiC_3-NH_3-H_2PW catalyst (entry 7). No significant improvement in the product yield and the reaction time was observed using higher amount of the catalyst. All subsequent reactions were carried out in these optimized conditions.

Table 1. Optimization of reaction parameters for the synthesis of compound **4b** catalyzed by GO-SiC_3-NH_3-H_2PW[a]

Entry	Catalyst (g)	Solvent	T (°C)	Time (min)	Isolated Yield (%)
1	-----	EtOH	Reflux	120	Trace
2	-----	H_2O	Reflux	120	Trace
3	-----	EtOH-H_2O	Reflux	120	Trace
4	-----	-----	120	120	Trace
5	0.01	EtOH	Reflux	40	43
6	0.02	EtOH	Reflux	30	74
7	0.03	EtOH	Reflux	15	90
8	0.04	EtOH	Reflux	20	89
9	0.03	H_2O	Reflux	30	48
10	0.03	EtOH-H_2O	Reflux	20	59
11	0.03	MeOH	Reflux	20	45
12	0.03	CH_3CN	Reflux	15	45
13	0.03	CH_2Cl_2	Reflux	15	57
14	0.03	$CHCl_3$	Reflux	15	52
15	0.03	-----	120	50	22

[a]Reaction conditions: *β*-naphthol **1** (1 mmol), 4-chlorobenzaldehyde **2b** (1 mmol), and acetamide **3** (1.2 mmol)

Using these optimized reaction conditions, the scope and efficiency of this approach was explored for the synthesis of amidoalkyl naphthols **4a-j** and the obtained results are summarized in Table 2. A wide range of *ortho*-, *meta*- and *para*-substituted aromatic aldehydes undergo one-pot multicomponent reaction with *β*-naphthol and acetamide under optimized conditions to afford amidoalkyl naphthol derivatives. The results showed that all electron-rich as well as electron-poor aromatic aldehydes reacted successfully and gave the products in high yields within short reaction time. The type of substituent on the aromatic aldehydes had no significant effect on the reaction time and yield. These results clearly indicate that the GO-SiC_3-NH_3-H_2PW acts as highly active catalyst in this methodology.

Table 2. Synthesis of amidoalkyl naphthols **4a-j** catalyzed by GO-SiC_3-NH_3-H_2PW[a]

Entry	Ar	Product	Time (min)	Isolated Yields (%)	m.p. (°C)	
					Found	Reported
1	C_6H_5	**4a**	20	88	239-241	241-243 [38]
2	4-ClC_6H_4	**4b**	15	90	227-229	228-229 [38]
3	3-ClC_6H_4	**4c**	12	86	238-240	237-238 [39]
4	2-ClC_6H_4	**4d**	20	82	211-212	212-214 [42]
5	4-BrC_6H_4	**4e**	15	91	228-230	230-232 [42]
6	4-MeC_6H_4	**4f**	15	89	216-218	213-215 [43]
7	4-$MeOC_6H_4$	**4g**	15	80	181-182	183-185 [43]
8	4-$O_2NC_6H_4$	**4h**	13	87	241-243	242-244 [43]
9	3-$O_2NC_6H_4$	**4i**	10	94	239-241	241-243 [43]
10	2-$O_2NC_6H_4$	**4j**	10	86	212-214	211-213 [44]

[a]Reaction conditions: *β*-naphthol **1** (1 mmol), an aromatic aldehyde **2a-j** (1 mmol), acetamide **3** (1.2 mmol), GO-SiC_3-NH_3-H_2PW (0.03 g), EtOH, reflux.

In view of the potential for green chemistry, the recycling performance of GO-SiC_3-NH_3-H_2PW was also investigated in the model reaction. Upon completion of the first run, the reaction mixture was filtered whilst still hot to separate the catalyst. The separated catalyst was washed with hot ethanol, dried at 70 °C under vacuum for 2 h, and reused in the subsequent catalytic runs. The recovered catalyst worked well for up to five catalytic runs without any significant loss of its activity (Figure 5) which clearly demonstrates the practical reusability of this catalyst.

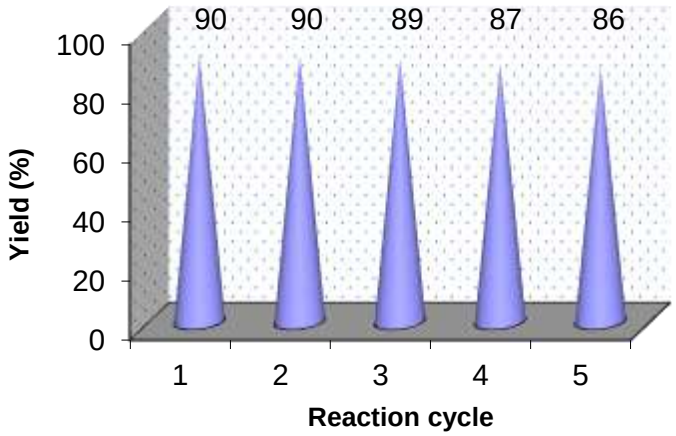

Figure 5. Reusability of GO-SiC_3-NH_3-H_2PW for the synthesis of compound **4b**

To show the catalyst's role, a plausible mechanism for this reaction may proceed as depicted in Scheme 3. As shown, *ortho*-quinone methide (*o*-QM) intermediate [**II**] is readily formed *in situ* by Knoevenagel condensation of *β*-naphthol **1** and aromatic aldehydes **2a-j** *via* the intermediate [**I**]. Subsequent, Michael addition of acetamide to the *o*-QM intermediate [**II**] afforded the final products **4a-j**. We believe that the catalyst GO-SiC_3-NH_3-H_2PW ≡ Cat. with several accessible W sites and P-O-H moieties can act as Lewis acid and Brønsted acid centres, respectively, and therefore activates the reactants and the intermediates in this reaction. However, under the reaction conditions used, attempts to isolate the intermediates failed.

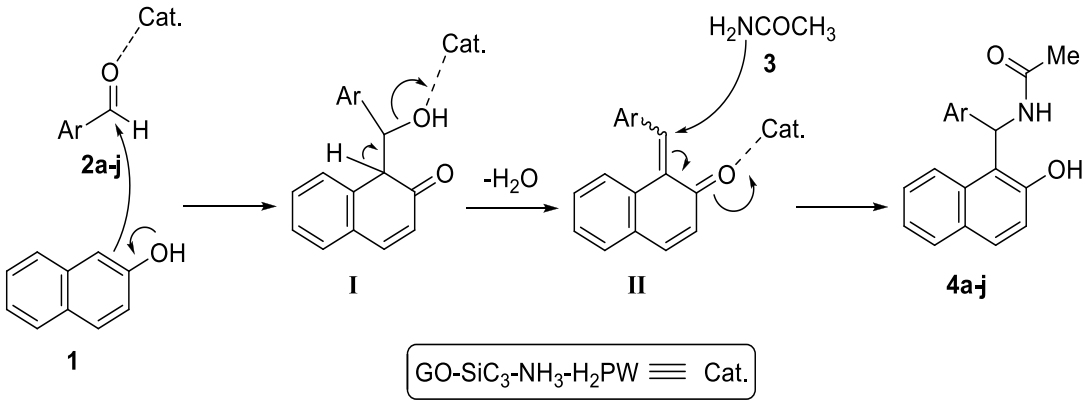

Scheme 3. Plausible mechanism for the formation of amidoalkyl naphthols in the presence of GO-SiC_3-NH_3-H_2PW as catalyst

Conclusion

In summary, a new functionalized GO containing a phosphomolybdic counter-anion, denoted as GO-SiC_3-NH_3-H_2PW, was successfully prepared by grafting of APTS on GO nanosheets followed by a reaction with H_3PW and, then, characterized using FT-IR spectroscopy, FESEM, EDX analysis, EDX elemental mapping, and ICP-OES. The new functionalized GO performed well as a catalyst in one-pot synthesis of amidoalkyl naphthols by reaction of *β*-naphthol with several aromatic aldehydes and acetamide in refluxing ethanol, giving high yields of the products within short reaction times. In addition, the catalyst is readily recovered by simple filtration and can be reused for subsequent reactions with no significant loss of its activity. Further applications of this new catalyst for other reaction systems are currently under investigation.

Acknowledgements

This work was supported by Islamic Azad University, Mashhad Branch (Iran) and Iran National Science Foundation.

References

[1] A.A. Balandin, S. Ghosh, W. Bao, I. Calizo, D. Teweldebrhan, F. Miao, C.N. Lau, *Nano Lett.*, **2008**, *8*, 902-907.
[2] S. Ghosh, S.R. Polaki, P.K. Ajikumar, N.G. Krishna, M. Kamruddin, *Indian J. Phys.*, **2018**, *92*, 337-342.
[3] D. Suhag, A. Kumar Sharma, S.K. Rajput, G. Saini, S. Chakrabarti, M. Mukherjee, *Sci. Rep.*, **2017**, *7*, Art. No. 537.
[4] O.C. Compton, S.T. Nguyen, *Small*, **2010**, *6*, 711-723.
[5] H. Chang, L. Tang, Y. Wang, J. Jiang, J. Li, *Anal. Chem.*, 2010, *82*, 2341-2346.
[6] M. Baghayeri, H. Alinezhad, M. Tarahomi, M. Fayazi, M. Ghanei-Motlagh, B. Maleki, *Appl. Surf. Sci*., **2019**, *478*, 87-93.
[7] (a) S. Mohammadi, A. Taheri, Z. Rezayati-zad, *Prog. Chem. Biochem. Res.*, **2018**, *1*, 1-10; (b) S. Sajjadifar, Z. Arzehgar, A. Ghayuri, *Journal of the Chinese Chemical Society*, **2018**, *65*, 205-211.
[8] Y. Shao, J. Wang, H. Wu, J. Liu, I.A. Aksay, Y. Lin, *Electroanalysis*, **2010**, *22*, 1027-1036.
[9] A.S. Mohamadhosein, S. Jamehbozorgi, J. Beheshtian, *Eurasian J. Anal. Chem.*, **2018**, *13*, Art. No. em28.
[10] M. Alem, A. Teimouri, H. Salavati, S. Kazemi, *Chem. Methodol.*, **2017**, *1*, 49-67.
[11] G. Vinodhkumara, R. Ramyab, M. Vimalanc, I. Vetha Potheherd, A. Cyrac Peter, *Prog. Chem. Biochem. Res.*, **2018**, *1*, 40-49.
[12] B. Tang, G. Hu, *J. Power Sources*, **2012**, *220*, 95-102.
[13] S. Khameneh Asl, M. Namdar, *Chem. Methodol.*, **2019**, *3*, 183-193.
[14] M. Yang, J. Yao, Y. Duan, *Analyst*, **2013**, *138*, 72-86.
[15] W.S. Hummers, R.E. Offeman, *J. Am. Chem. Soc.*, **1958**, *80*, 1339-1339.
[16] X. Zheng, W. Hou, Q. Lian, H. Wu, *Russ. J. Gen. Chem.*, **2016**, *86*, 915-918.
[17] H.J. Shin, K.K. Kim, A. Benayad, S.M. Yoon, H.K. Park, I.S. Jung, M.H. Jin, H.K. Jeong, J.M. Kim, J.Y. Choi, Y.H. Lee, *Adv. Funct. Mater.*, **2009**, *19*, 1987-1992.
[18] S. Stankovich, D.A. Dikin, R.D. Piner, K.A. Kohlhaas, A. Kleinhammes, Y. Jia, Y. Wu, S.T. Nguyen, R.S. Ruoff, *Carbon*, **2007**, *45*, 1558-1565.
[19] S. Bhattacharya, P. Ghosh, B. Basu, *Tetrahedron Lett.*, **2018**, *59*, 899-903.
[20] H. Alinezhad, M. Tarahomi, B. Maleki, A. Amiri, *Appl. Organometal. Chem.*, **2019**, *33*, Art. No. e4661.

[21] J. Zhang, Y. Yang, J. Fang, G.-J. Deng, H. Gong, *Chem. Asian J.*, **2017**, *12*, 2524-2527.
[22] M. Shaikh, S.K. Singh, S. Khilari, M. Sahu, K.V.S. Ranganath, *Catal. Commun.*, **2018**, *106*, 64-67.
[23] D.R. Dreyer, S. Park, C.W. Bielawski, R.S. Ruoff, *Chem. Soc. Rev.*, **2010**, *39*, 228-240.
[24] J. Zhao, Y. Xie, J. Fang, Y. Ling, Y. Gao, X. Liu, Q. Zhang, Q. Xu, H. Xiong, *J. Mater. Sci.*, **2016**, *51*, 10574-10584.
[25] J. Zhao, Y. Xie, D. Hu, D. Guan, J. Chen, J. Yu, S. He, Y. Lü, H. Liu, S. Bao, L. Wang, *Synth. Met.*, **2015**, *204*, 95-102.
[26] M.R. Majidi, S. Ghaderi, *Iran. Chem. Commun.*, **2018**, *6*, 242-255.
[27] B. Konkena, S. Vasudevan, *Langmuir*, **2012**, *28*, 12432-12437.
[28] M. Cano, U. Khan, T. Sainsbury, A. O'Neill, Z. Wang, I.T. McGovern, W.K. Maser, A.M. Benito, J.N. Coleman, *Carbon*, **2013**, *52*, 363-371.
[29] S. Stankovich, R.D. Piner, S.T. Nguyen, R.S. Ruoff, *Carbon*, **2006**, *44*, 3342-3347.
[30] S. Verma, M. Aila, S. Kaul, S.L. Jain, *RSC Adv.*, **2014**, *4*, 30598-30604.
[31] H. Su, Z. Li, Q. Huo, J. Guan, Q. Kan, *RSC Adv.*, **2014**, *4*, 9990-9996.
[32] B.B. Touré, D.G. Hall, *Chem. Rev.*, **2009,** *109*, 4439-4486.
[33] R. Javahershenas, J. Khalafy, *Asian J. Green Chem.*, **2018**, *2*, 318-329.
[34] R. Motamedi, F. Ebrahimi, G. Rezanejade Bardajee, *Asian J. Green Chem.*, **2019**, *3*, 22-33.
[35] S. Sajjadifar, I. Amini, H. Jabbari, O. Pouralimardan, M.H. Fekri, K. Pal, *Iran. Chem. Commun.*, **2019**, *7*, 191-199.
[36] A. Hassankhani, *Iran. Chem. Commun.*, **2019**, *7*, 248-256.
[37] H. Hasani, M.Irizeh, *Asian J. Green Chem.*, **20**18, *2*, 85-95.
[38] L. Nagarapu, M. Baseeruddin, S. Apuri, S. Kantevari, *Catal. Commun.*, **2007**, *8*, 1729-1734.
[39] J. Luo, Q. Zhang, *Monatsh. Chem.*, **2011**, *142*, 923-930.
[40] W.-Q. Jiang, L.-T. An, J.-P. Zou, *Chin. J. Chem.*, **2008**, *26*, 1697-1701.
[41] M. Lei, L. Ma, L. Hu, *Tetrahedron Lett.*, **2009**, *50*, 6393-6397.
[42] S. Sheik Mansoor, K. Aswin, K. Logaiya, S.P.N. Sudhan, *J. Saudi Chem. Soc.*, **2016**, *20*, 138-150.
[43] A.R. Kiasat, L. Hemat-Alian, S.J. Saghanezhad, *Res. Chem. Intermed.*, **2016**, *42*, 915-922.
[44] S. Puri, B. Kaur, A. Parmar, H. Kumar, *Org. Prep. Proced. Int.*, **2012**, *44*, 91-95.
[45] (a) M. Kooti, M. Karimi, E. Nasiri, *J. Nanopart. Res.*, **2018**, *20*, Art. No. 16; (b) Z. Arzehgar, S. Sajjadifar, H. Arandiyan, *Asian J. Green Chem.*, **2019**, *3*, 43-52.
[46] B. Maleki, E. Sheikh, E.R. Seresht, H. Eshghi, S.S. Ashrafi, A. Khojastehnezhad, H. Veisi, *Org. Prep. Proced. Int.*, **2016**, *48*, 37-44.
[47] A. Davoodnia, M. Khashi, N. Tavakoli-Hoseini, *Chin. J. Catal.*, **2013**, *34*, 1173-1178.
[48] M. Khashi, A. Davoodnia, V.S. Prasada Rao Lingam, *Res. Chem. Intermed.*, **2015**, *41*, 5731-5742.
[49] M. Rohaniyan, A. Davoodnia, A. Nakhaei, *Appl. Organomet. Chem.*, **2016**, *30*, 626-629.
[50] A. Davoodnia, A. Nakhaei, N. Tavakoli-Hoseini, *Z. Naturforsch.*, **2016**, *71b*, 219-225.
[51] S. Ameli, A. Davoodnia, M. Pordel, *Org. Prep. Proced. Int.*, **2016**, *48*, 328-336.
[52] M. Fattahi, A. Davoodnia, M. Pordel, *Russ. J. Gen. Chem.*, **2017**, *87*, 863-867.
[53] F. Tajfirooz, A. Davoodnia, M. Pordel, M. Ebrahimi, A. Khojastehnezhad, *Appl. Organometal. Chem.*, **2018**, *32*, Art. No. e3930.
[54] A. Nakhaei, A. Davoodnia, S. Yadegarian, *Iran. Chem. Commun.*, **2018**, *6*, 334-345.

[55] E. Teymooria, A. Davoodnia, A. Khojastehnezhad, N. Hosseininasab, *Iran. Chem. Commun.*, **2019**, *7*, 271-282.

How to cite this manuscript: Zahra Hoseini, Abolghasem Davoodnia, Amir Khojastehnezhad, Mehdi Pordel. Phosphotungstic acid supported on functionalized graphene oxide nanosheets (GO-SiC_3-NH_3-H_2PW): Preparation, characterization, and first catalytic application in the synthesis of amidoalkyl naphthols. *Eurasian Chemical Communications*, 2020, 2(3), 398-409.